Electrochemical Hydrogen Evolution by Cobalt (II) Porphyrins: Effects of Ligand Modification on Catalytic Activity, Efficiency and Overpotential

Belete B. Beyene,[1,2] Sandeep B. Mane,[1] and Chen-Hsiung Hung [1,*,z]

[1] *Institute of Chemistry, Academia Sinica, Nankang, Taipei 11529, Taiwan*
[2] *Department of Chemistry, Bahir Dar University, Bahir Dar, Ethiopia*

Electrochemical H_2 evolution of a series of cobalt(II) porphyrins with electron-withdrawing (EW) and electron-donating (ED) substituents at the *para* positions of the *meso*-phenyl rings has been investigated in DMSO using acetic acid as a proton source. Our study showed that the nature of substituents significantly influences catalytic activity, efficiency, and the potential at which catalysis occurs. Faradaic efficiencies (FE) ranging from 44 to 99%, turnover numbers (TONs) from 1.5 to 104 (∼11 h electrolysis), turnover frequencies (TOFs) from 0.23 to 9.1 h^{-1}, and onset overpotentials from 25 to 445 mV were obtained by tuning the porphyrinic substituents. Cobalt porphyrins with -SO_3H, -COOH, or -NH_2 groups as the substituents showed high activity and efficiency with more positive onset potentials as compared to the parent [Co(TPP)]. Supports also from the low hydrogen generation activities for complexes with -COOMe, -OMe and -OH groups as the substituents suggest that the acidity of the *meso*-phenyl substituent plays a key role in enhancing the hydrogen evolution activities during the catalytic processes.

[DOI: 10.1149/2.0481809jes]

Manuscript submitted March 5, 2018; revised manuscript received May 14, 2018. Published June 8, 2018. This was Paper 875 presented at the New Orleans, Louisiana, Meeting of the Society, May 28–June 1, 2017.

Hydrogen has emerged as an attractive candidate for clean and sustainable fuel.[1,2] Despite the simplest covalent bond, the thermodynamic and kinetic barriers for generating H_2 without the presence of a catalyst are very high.[3] Over the past few years, cobalt complexes of various macrocycles have been extensively studied and used as catalysts for H_2 generation either in aqueous or non-aqueous medium under acidic conditions both in heterogeneous and homogenous systems.[4–10] Cobaltous porphyrin complexes are also among the most fascinating compounds to be employed in H_2 evolution.[11] The first study dealing with cobalt porphyrins as H_2 evolving catalysts was reported in 1985 by Kellett and Spiro.[12,13] However, the activity was observed through adsorption of metalloporphyrins to the electrode surface, which hampers a thorough kinetic and mechanistic investigation. In 1998, [Co(TPP)] (where, TPP = 5,10,15,20-tetraphenylporphyrinato) has been reported to serve as a heterogeneous electrocatalyst in a pH 1 aqueous solution by incorporating it to a Nafion membrane coated on a Pt electrode.[14] Nocera and co-workers also intensively studied electrochemical H_2 generation using cobalt(II) hangman porphyrins as the catalyst in the presence of benzoic and tosic acids in acetonitrile.[11,15,16] Their works provide essential insights into the H_2 evolving mechanism, proton transfer rate constants, and the roles of hanging group in lowering the overpotential. Lately, photocatalytic and heterogeneous H_2 generation using water-soluble cationic $[Co^{II}(NMeTPyP)]^{4+}$ (where, NMeTPyP = meso-tetrakis(1-methyl-pyridinium-4-yl)-porphyrin) was studied.[17–19] Electrochemical H_2 evolution using highly active water-soluble biomolecular catalyst made from cobalt substitution of micro-peroxidase-11 was studied in homogenous solution.[9] Quite recently, we have reported the use of water-soluble cobalt(II) *meso*-(tetraphenyl-4-sulfonato)porphyrin as a highly efficient, active, and stable catalyst for H_2 evolution in neutral phosphate buffer solution under electrochemical conditions.[20] This success inspired us to explore the potential roles of peripheral functional groups on the porphyrin core to the catalytic activity.

A key advantage of a well-defined molecular catalyst lies in the possibility of tuning its performance via synthetic chemistry. Functionalization or ligand modification of cobalt-based electrocatalysts to tune their catalytic activity and electrochemical property has been well studied and going rapidly.[21–23] Although the parent [Co(TPP)] and its derivatives have been reported as effective electrocatalysts for H_2 generation, it is still required to optimize their catalytic performance and onset overpotential in order that a low-cost and large-scale hydrogen production can be achieved. In this study, the substituents at the *para* positions of the *meso*-phenyl rings were varied from EW groups (-COOMe [1], -COOH [2] and -SO_3H [3]), -H [4] (i.e., unsubstituted phenyl), to ED groups (-NH_2 [5], -OH [6], and -OMe [7]) (Scheme 1). To ensure consistent experimental conditions, we choose DMSO as the solvent, in which all the molecules are readily soluble and acetic acid was used as an inexpensive organic proton source. The catalytic activity parameters such as FE, TON, TOF and onset overpotential were determined by using the combination of electrochemical methods followed by gas chromatography. Our results showed that ligand modification considerably affects the catalytic activity, efficiency and onset overpotential of electrocatalytic H_2 generation. In line with this, complexes **2**, **3**, and **5** are much more active and efficient catalysts with low onset potentials for generating H_2 as compared to the parent molecule **4**. On the other hand, complexes **1**, **6**, and **7** were observed to evolve very less amount of H_2 at an applied potential of −1.6 V *vs* NHE.

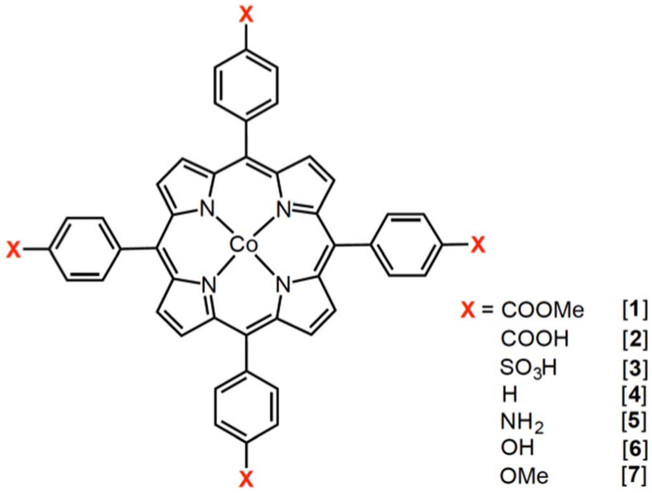

Scheme 1. Molecular structures of cobalt(II) porphyrins.

Materials and Methods

Synthesis and characterization.—The *meso*-5,10,15,20-tetraphenylporphyrins were prepared by following reported

---

*Electrochemical Society Member.
[z] E-mail: chhung@gate.sinica.edu.tw

procedures[24–28] via condensation reactions of the corresponding benzaldehyde with pyrrole in a mixed solvent of propionic acid and acetic anhydride. The amino functional group was obtained by reduction of nitro group using $SnCl_2$/HCl. Carboxyl group was prepared by base-catalysed hydrolysis of ester functionality. A subsequent cobalt metalation using $Co(OAc)_2 \bullet 4H_2O$ as the metal salt in DMF under reflux conditions afforded the desired cobalt complexes. The free base porphyrins and complexes were characterized by spectroscopic techniques as shown in supporting information (SI).

Electrochemical and catalytic study.—Cyclic voltammetry of 0.5 mM of complexes in 0.1 M $[Bu_4N]PF_6$/DMSO solution was recorded at different scan rates. The dependence of cathodic current peak on scan rate was deduced from cyclic voltammetry (CV) for all complexes. Electrocatalytic H_2 evolution activity of the complexes was measured by carrying out CV, amperometry (IT), and differential pulse voltammetry (DPV) experiments in the presence of proton source. To DMSO solution containing 0.1 M $[Bu_4N]PF_6$ electrolyte in three electrode systems, was added 0.5 mM catalysts and 80 equivalents of acetic acid and then the CV, DPV and IT were recorded.

Controlled-potential electrolysis (CPE).—Controlled-potential electrolysis experiments were conducted in a sealed cell with three electrode system, glassy carbon as the working, silver wire as reference, and platinum as auxiliary electrodes, in 10 mL of 0.1 M $[nBu_4N]PF_6$/ DMSO with 0.5 mM catalysts and 160 mM AcOH. The extended CPE experiments of all complexes were lasted for 11 h at −1.6 V vs NHE indicating their stability under electrolysis condition. The evolution of H_2 was confirmed by analysis of the headspace of the reaction mixture with GC following CPE experiment. The amount of H_2 evolved was quantified and used to determine catalytic performance parameters.

Determination of catalytic performance parameters.—*Onset overpotential*.—Onset overpotential is a potential difference between thermodynamic reduction potential of acetic acid in DMSO and the onset potential (the potential at which catalysis starts to occur).[29] From CV and LSV experiments, onset overpotentials of all complexes were estimated.

Faradaic efficiency.—One of the attribute for a good catalyst is high efficiency, exhibited in the case of electrochemistry by large catalytic currents for given concentrations of catalyst in the presence of excess acid under similar experimental conditions as determined by Evans and Glass.[21] It is the ratio of amount of hydrogen produced practically (as determined by GC using calibration curve of standard H_2) and theoretical yield obtained from bulk electrolysis. Thus, under similar experimental condition, their faradaic efficiency toward proton reduction was determined.

Catalytic activity and stability.—TON and TOF are related to the amount of hydrogen produced in practical (from GC) per amount of catalyst used for study. Both TON and TOF of all complexes were measured after 11 h controlled potential electrolysis in the presence of catalyst and excess proton source.

Results and Discussion

Synthesis and electronic spectra.—The synthesis of the desired free-base porphyrins follows procedures from the condensation of pyrrole with a corresponding aldehyde.[24,25] The spectroscopic properties of the obtained products are identical with those reported in literature. Alder's method was then used to insert the cobaltous ion into the central cavity of the porphyrin core. Despite variations in the wavelengths of absorption peaks, the common UV-vis absorptions featuring a *Soret* and several Q bands were observed for all ligands. The absorption patterns have changed as a result of cobalt metalation, with the most remarkable difference being the decrease on the number of Q band.[30] Moreover, based on experimental results, the nature of the functional groups influences UV-vis absorption of the studied compounds (Figure 1). In addition, many factors affect the absorption band of porphyrins. For instance, the electronic and steric nature of substituents, effect of solvent and capability of self-aggregation of substituent. Accordingly, the electron rich substituent such as NH_2 and OH groups, contributed to the 18 π-electron systems due to the resonance effect and red-shifted the absorption bands as compared to other substituents. Moreover, they can self-aggregate, which might also contribute to the observed bathochromic shift. For complexes with electron withdrawing COOH and SO_3H groups, hypsochromic shift is expected. However, likely because of self-aggregation, the absorption band shifted to longer wavelength as compared to parent Co(TPP), **4**.[31] The *Soret* bands of COOMe and OMe substituted cobalt complexes are close to parent molecule.

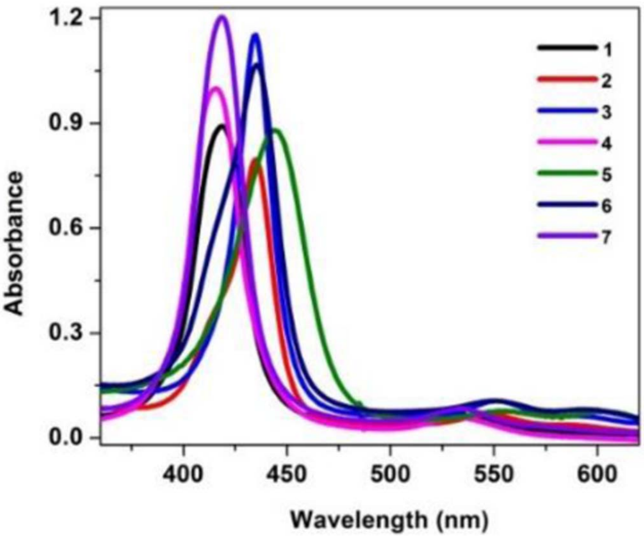

Figure 1. Absorption spectra of studied complexes in DMSO.

Upon addition of excess acetic acid to the DMSO solution of catalysts, blue-shift was observed only in the solution of compound **5**, which is consistent with protonation of amino groups to yield an active catalyst containing terminal EW $-NH_3^+$ groups (Fig. 2). It thus supports that under acidic electrocatalysis, the active form involving in catalytic processes is the porphyrin with $-NH_3^+$ functional groups. The absorption patterns of all the rest catalysts did not change because of addition of the proton source (Fig. SI 24), suggesting stable cobalt(II) porphyrins under acidic conditions.

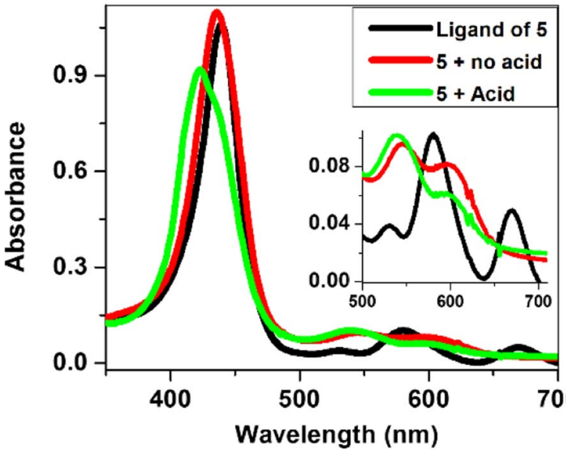

Figure 2. Absorption spectra of complexes **5** and its ligand in DMSO with or without the addition of acetic acid.

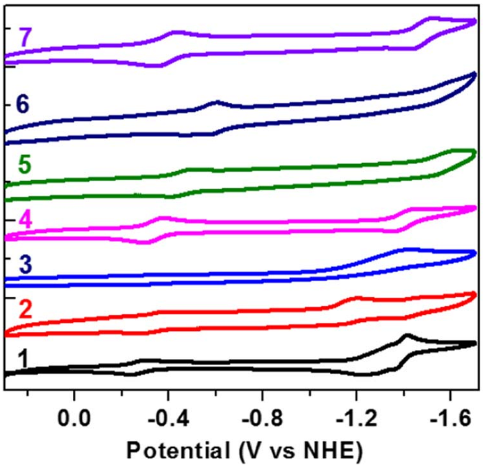

Figure 3. Cyclic voltammograms of 0.5 mM of cobalt(II) porphyrin complexes in 0.1 M $[Bu_4N]PF_6$/DMSO at scan rate of 0.1 V/s using glassy carbon working electrode at room temperature.

Electrochemical and catalytic study.—Electrochemical studies showed that the redox potentials of cobalt(II) porphyrins with the substituent on each of the *meso*-phenyl ring, are highly tuneable. As expected, the potentials of the first $Co^{2+/1+}$ and the second $Co^{1+/0}$ redox couples both changed systematically with the electronic nature of the substituents. The potentials were measured with reference to Ag/AgCl and converted to NHE by adding 0.21 V to the measured potentials.[32,33] The CV measurement using a glassy carbon working electrode in DMSO and 0.1 M tetra-*n*-butylammonium hexafluorophosphate, $[Bu_4N]PF_6$ as the supporting electrolyte showed electrochemically reversible redox processes at potentials (vs. NHE) ranging from −0.27 to −0.59 for $Co^{2+/1+}$ and −1.34 to −1.58 V for $Co^{1+/0}$ (Fig. 3).

The complex with the EW -COOMe substituents exhibits the least negative $Co^{2+/1+}$ and $Co^{1+/0}$ reduction potentials (−0.27 and −1.34 *vs.* NHE). The congener with the ED -OH group has shifted to the most negative potential (−0.59 V and −1.58 V vs. NHE), revealing substantial electronic communication through the porphyrin ligand to the metal center.

Upon addition of AcOH to the solution of cobalt complexes in DMSO, catalytic current dramatically enhanced at the potential close to the $Co^{1+/0}$ redox couple, with onset potentials varying from −0.955 to −1.38 V vs NHE. For complex **5**, however, the catalytic peak appeared at a potential much less negative than that of $Co^{1+/0}$ pair measured in the absence of AcOH, which is consistent with an electron deficient metal center resulted from the protonation of amino group to $-NH_3^+$. As can be seen from linear sweep voltammetry (LSV) in Figure 4, the magnitudes of catalytic current enhancement and onset potential vary with the most positive shift and highest catalytic current enhancement being for complex **3** with terminal sulfonates, which suggests an efficient proton delivery at favorable applied potential. It is about 320 mV less negative than the parent molecule and 420 mV positive shift when compared to complex **6** (the most negative onset potential) as determined from CV and LSV.

Scanning to more negative potentials in the presence of excess AcOH resulted in the sharp increase in current, indicative of electrocatalytic proton reduction and H_2 generation as also confirmed from GC chromatograms. Such subsequent sharp rise in current at lower onset potential in the presence of excess protons (Fig. 5 and SI 27-30) highly depends on the acidity and electronic properties of the functional groups. This implies that substitutions in fact do adjust the potential at which catalysis arises (onset potential). Control experiments employing cobalt acetate in the presence of 160 mM AcOH showed no catalytic activity at the potential ranges where catalyst operates. Moreover, catalytic activities of porphyrinic ligands of **2**, **3**, **5** and **6**, without the cobalt(II) ion, were examined in the presence of 160 mM AcOH. Except ligand of **2**, which showed some catalytic activity, all others showed no catalytic activity at all (Fig. 5a). Thus, an increase in catalytic current is due to the catalytic cycles that produce molecular hydrogen. It is also apparent that, acidification didn't affect $Co^{2+/1+}$ reduction feature of all complexes, indicating that protonation of Co^0 presumably yields cobalt(II)-hydride as a reactive intermidate.[30] In principle, the Co(II)-H intermediate formed upon protonation of Co^0, can readily generate H_2 under acidic conditions. Supported by control experiments, the enhancement on current peak is not due to a direct reduction of acetic acid.

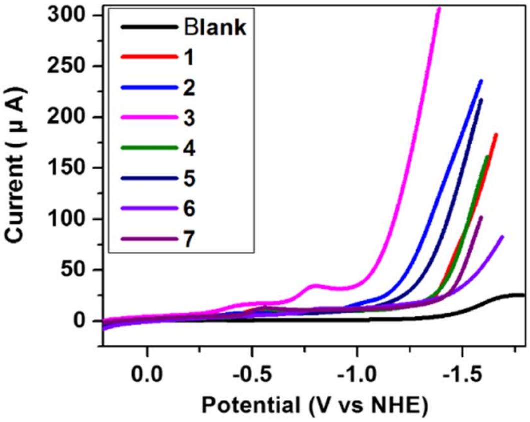

Figure 4. Linear sweep voltammograms of 0.5 mM of complexes in the presence of 160 mM AcOH/DMSO containing 0.1 M $[Bu_4N]PF_6$ using glassy carbon electrode. Control experiment using AcOH alone (160 mM, black) was also displayed.

To assess faradaic efficiency and TOF of H_2 evolution, controlled potential electrolysis of 0.5 mM solution of cobalt complexes was conducted at −1.6 V vs NHE for 11 h in the presence of 160 mM AcOH in 10 mL of DMSO (Fig. 6) and quantified H_2 produced by GC. Although an increase in charge with time is clearly observed for all of the complexes, the amount of charge accumulation per second varies depending on the inherent activity of catalyst toward proton reduction. Significant increment was noticed for complex **3**, followed by **2** and **5**, when the electrolysis was conducted for 11 h. Moreover, CPE experiments of blank acetic acid show insignificant catalytic activity under the same experimental conditions. Following CPE experiment, the headspace gas mixture was analyzed by GC (Fig. 7) and the amount of H_2 generated was quantified (Fig. 8) using calibration curve of standard H_2. The TOF, FE, and TON are deduced from CPE experiment at a potential of −1.6 V *vs* NHE, in which charge ranging from 17.8 to 101 C was passed during electrolysis.

Comparison of catalytic performance parameters.—Analysis of the headspace by gas chromatography following electrolysis for around 11 h at −1.6 V (vs NHE) obtained parameters of the catalytic performance such as onset overpotential (E_{ovp}), FE, TON, and TOF. Large diversity on the catalytic performance were observed by tuning the substituents on the porphyrin core with faradaic efficiencies (FE) ranging from 44 to 99.4%, TONs from 1.5 to 104, TOFs from 0.23 to 9.12 h^{-1}, and E_{ovp} from 25 to 445 mV (Table I). The trends of these parameters are consistent with catalytic current enhancements and onset potential features observed in CV, LSV and DPV experiments under acidic conditions. Therefore, such a significant variation reveals an important role of the functional groups on tuning the catalytic activity.

Even though it is anticipated that molecules with strong electron-donating groups have more negative redox potentials due to the more electron-rich metal center and porphyrin core and are expected to be more active toward H_2 generation, the −1.6 V (vs NHE) of applied potential in this study wasn't negative enough to produce a large amount of H_2 in the cases of complexes **6** and **7**. Moreover, for most of the earth-abundant transition metal molecular catalysts reported to

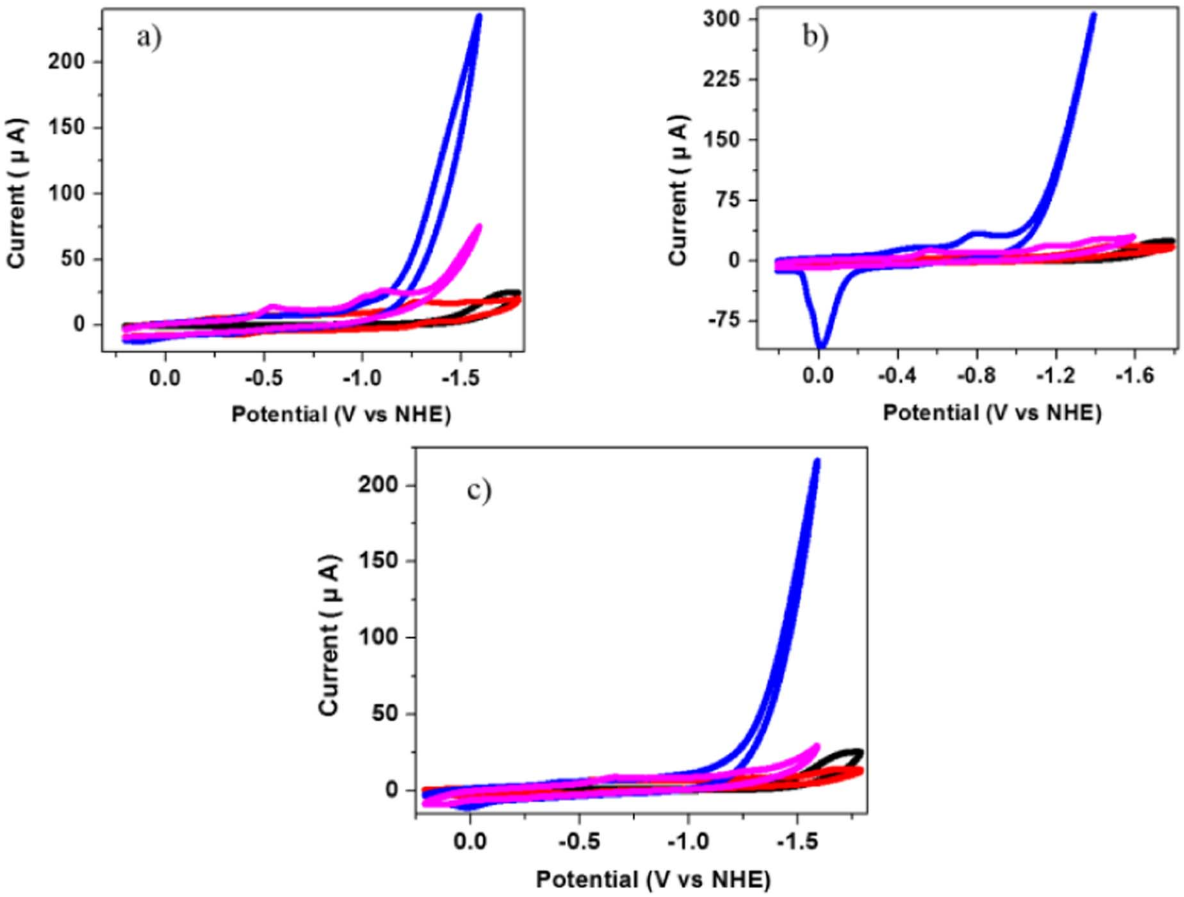

Figure 5. Cyclic voltammograms of 0.5 mM of active complexes: a) **2**, b) **3** and c) **5** in the presence of 160 mM AcOH/DMSO containing 0.1 M $[Bu_4N]PF_6$ using glassy carbon electrode. Catalyst with 160 mM AcOH (blue), control experiment using 160 mM AcOH alone (black), catalyst with no acid (red), and ligand only with 160 mM acid (magenta).

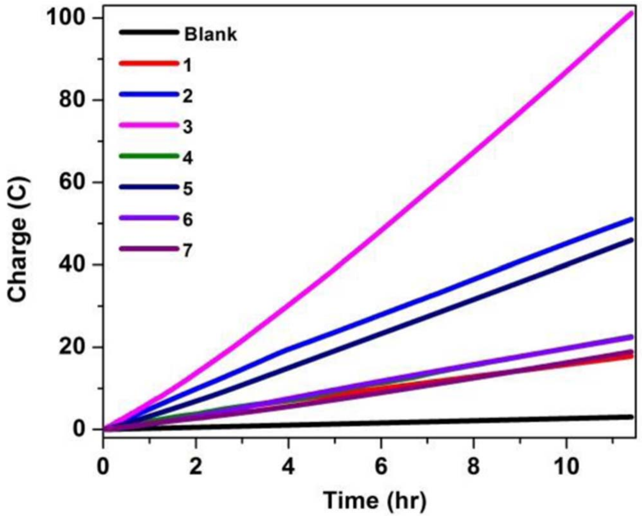

Figure 6. Controlled potential electrolysis for 11 h for 0.5 mM complexes in the presence of 160 mM AcOH/DMSO solution at –1.6 V *vs* NHE.

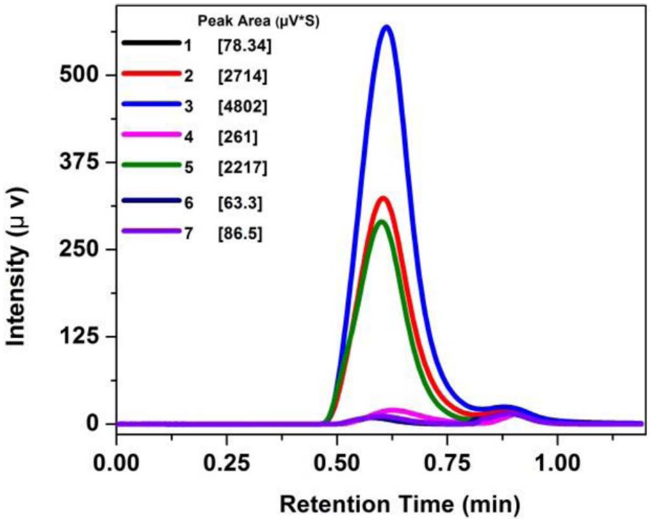

Figure 7. Gas chromatograms after 11 h for 0.5 mM complexes in the presence of 160 mM AcOH/DMSO solution at –1.6 V *vs* NHE.

date, high activity is observed when more negative potential is applied and catalysts working at low applied potential usually display low catalytic activities. However, in this particular study highest catalytic activity with faradaic efficiency of 99.4%, TOF of 9.12 h^{-1}, and a TON of 104 (after 11 h) was observed using **3** as the catalyst even though **3** has the lowest overpotential, i.e. the least negative onset potential. Such an unusual trend of increasing catalytic activity with a less negative onset potential, suggests that a higher catalytic activity can be achieved through molecular design. In our case, analysis of the correlations of molecular structure and catalytic activities showed that the combination of factors such as the presence of an acidic proton on ligand, electron withdrawing nature of substituents and

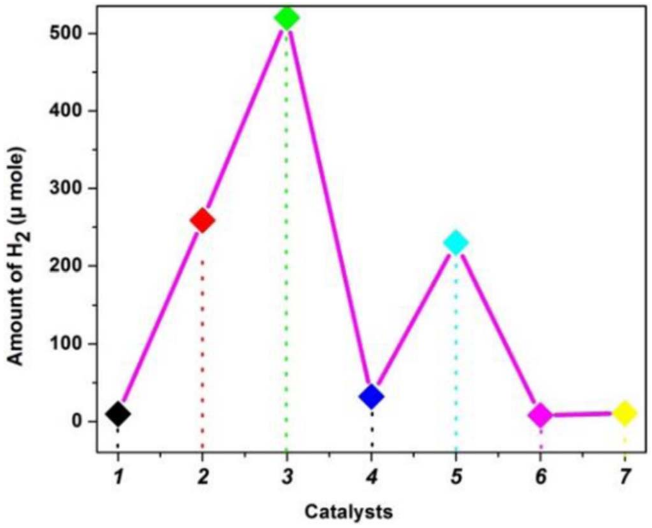

Figure 8. The amount of H_2 produced after 11 h electrolysis of 0.5 mM complexes in the presence of 160 mM AcOH/DMSO solution at – 1.6 V *vs* NHE as determined from GC (Figure 8).

surface anchoring moiety of the catalysts significantly enhances the H_2 evolution activity.

Even though a catalyst with a more negative onset potential, i.e. a larger overpotential resulted from a relative electron rich catalytic center is expected to be favourable for electrochemical H_2 generation, we have confirmed that higher rates of catalysis can be achieved without increasing overpotential. Bullock and co-workers also reported similar observations in which fastest turnover frequencies for H_2 generation from acetic acid in acetonitrile using Ni(diphosphine)$_2^{2+}$ complexes with electron withdrawing groups.[3] In this report, the low catalytic activity of a catalyst with –COOMe as the terminal functional groups, which gave a TOF of only 0.23 h^{-1}, further confirmed that the electronic property will not be the dominant and the only factor. Instead, due to the lacking of any acidic proton and surface anchoring group, the efficiency of this catalyst is much lower than the catalyst containing terminal carboxylic acid as the substituent.

Noticeably, although catalyst **5** is a compound with a relative negative redox potential for $Co^{2+/1+}$ and $Co^{+1/0}$ couple in CV measurements in the absence of an acid, the onset overpotential for H_2 evolution is relatively positive in the presence of AcOH as the proton source. This discrepancy is presumably due to the protonation of amino group to form $-NH_3^+$ under acidic conditions as evidence from UV-visible absorption and CV measurements. Thus, the relative active behavior of catalyst **5** is more related to protonation of amino group in AcOH to offer a strong acid for H_2 evolution but not the ED characteristic of $-NH_2$. Since studies on electrochemical H_2 production were made in different media using various acids with different working and reference electrodes, it is difficult to evaluate the efficiencies of electrocatalysts by directly comparing the TOF and catalytic potentials observed in different research groups. Nevertheless, literature reported electrocatalytic H_2 production by cobalt-based catalysts with strong and moderate acids as proton sources in different organic solvents showed catalytic onset potentials ranging from −0.07 V to −1.84 V *vs* NHE, faradaic efficiencies from 10 to 100% and TONs from < 0.5 to 90 h^{-1} at applied overpotentials ranging from 0 to 830 mV.[33,34] Thus, moderate to good catalytic activities, efficiencies, and onset potentials are obtained in this report with catalyst **3** listed as one of the best catalysts among all available porphyrin-based catalysts with electrochemical H_2 evolution activities. Most importantly, our results illustrate the importance of tuning the functionality of the *meso*-phenyl ring to achieve optimized rates of catalysis. Based on our experimental result, the catalytic activity order of the complexes in DMSO/AcOH is **3**> **2**>**5** > **4** > 7~**6**~**1**.

Mechanistic approach in AcOH/DMSO.—The mechanism of electrochemical H_2 evolution by Co(II) molecular catalysts in weak proton sources involves a two-step $1e^-$ reduction of Co^{2+} to Co° followed by protonation of Co^0 to form Co(II)-hydride as a reactive intermediate.[5,15,17,39,40] We also reported a mechanism for electrocatalytic H_2 evolution employing Co(II) porphyrin as a catalyst in H_2O (weak proton source)[20] and based on similar spectroscopic and CV results all the Co(II) porphyrins presented here follow a resemble mechanism as shown in Scheme 2. But, in the case of catalyst **5** with *para*-NH_2 substitution, protonation of amino group may occur first to give $-NH_3^+$, which will take part in catalysis.

Electrocatalytic study in neutral water.—Encouraged by enhanced homogenous catalytic activity of **2**, **3** and **5** in organic solvents, we extended our study to heterogeneous electrochemical H_2 generation in neutral water by electrochemically modifying glassy carbon electrode in the catalysts solution using continuous CV sweep (from 0 to −1.5V vs NHE, 50 cyclecs) and then extended electrolysis at −1.5 V vs NHE for 2h. Only, the active catalysts in organic solvent have been used for electrode modification and electrocatalytic

Table I. Electrocatalytic H_2 production by cobalt(II) porphyrins with AcOH as proton source.

Catalyst	E_{onset} (V vs NHE)	J_{max} (mA/cm^2)	$E_{onset\ OP}$ (mV)	TON (~11 h)	TOF (h^{-1})	FE %
1	−1.23	1.93	295	1.9	0.23	54.3
2	−1.13	3.6	197	51.8	4.54	98.1
3	−0.96	8	25	104.1	9.12	99.4
4	−1.29	1.8	355	6.4	0.56	47
5	−1.22	3.4	285	46	4.04	95.8
6	−1.38	0.73	445	1.5	0.31	47.7
7	−1.36	1.2	425	2.1	0.32	43.8

CH_3COOH in DMSO (pKa = 12.6, E^0 (HA/H_2) = −0.93 V *vs* NHE). During bulk electrolysis, −1.6 V *vs* NHE was applied. $E_{onsetOP} = E^0_{HA}$ - E_{cat}, where E^0_{HA} is thermodynamic potential and E_{cat} is potential at which catalysis starts to occur. J_{max} is current density.

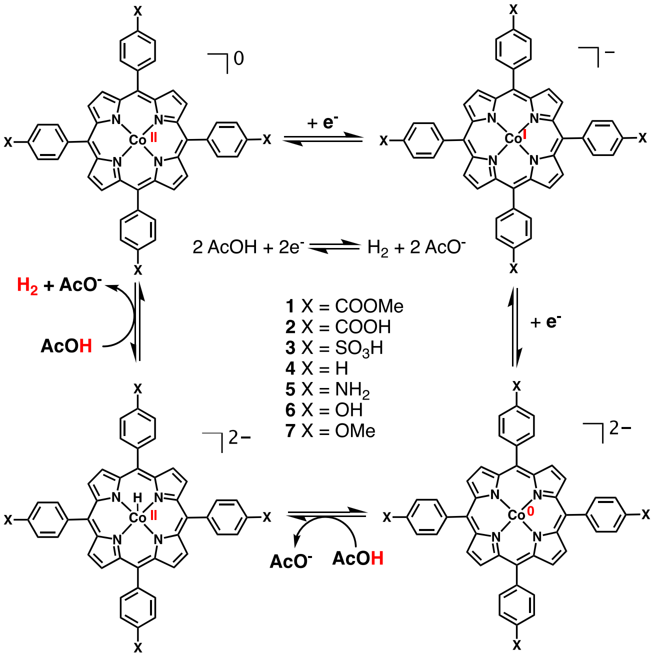

Scheme 2. Mechanism of H_2 evolution of catalysts in the presence of AcOH in DMSO.

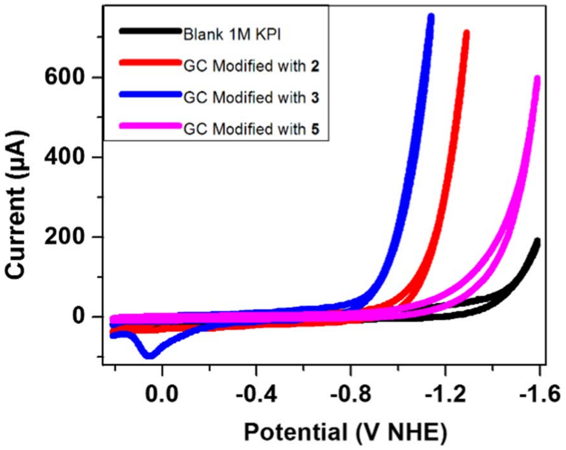

Figure 9. Cyclic voltammograms in neutral aqueous solution (1 M KPi, pH 7) using glassy carbon electrode coated with catalyst **2**, **3**, or **5** as the working electrode.

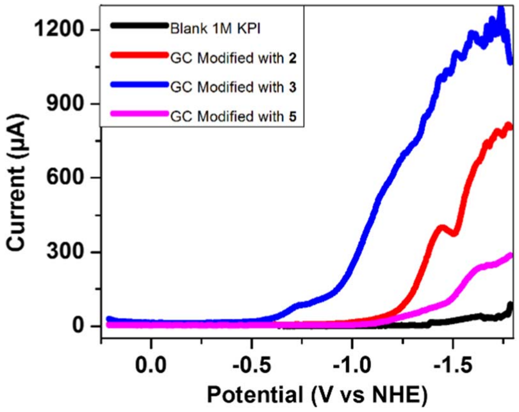

Figure 10. Differential pulse voltammograms in neutral aqueous solution (1 M KPi, pH 7) using catalyst **2**, **3**, or **5** coated glassy carbon as the working electrode.

H_2 generation ability was evaluated in neutral aqueous solution (1 M KPi, pH 7). Based on CV, DPV, controlled-potential electrolysis and GC experiments, the catalysts have ability to generate H_2 from neutral water, with the activity of **3** still higher than others (Figs. 9, 10).

Conclusions

In summary, electrocatalytic H_2 generation activity of a series of cobalt(II) porphyrins with EW and ED substituents on *meso*-phenyl rings have been investigated. The nature of substituents has played an important role in amending efficiency, catalytic activity and the potential at which catalysis occurs. Upon applying a potential of −1.6 V vs NHE, enhanced catalytic activity and efficiency was observed for **2**, **3** and **5** at less negative onset potential when compared to either parent molecule or other studied molecules. Such unexpected trends of increasing catalytic activity and efficiency with more positive onset potentials show that higher rates of catalysis can be achieved without increasing overpotential. The key factors in enhancing catalytic activity and lowering onset overpotential are found to be the combination of acidity of the functional group, electron withdrawing nature and surface anchoring moiety at *para* position of *meso*-phenyl rings. This study set a direction for future optimization and further modification of porphyrin macrocycles for electrocatalytic H_2 generation in organic solvents or in aqueous phase under both electrochemical or photocatalytic approaches using either homogeneous or heterogeneous catalysts. The complexes employed in current work are advantageous because of their capability in catalyzing hydrogen evolution from both organic acid as homogenous catalytic systems and water as heterogeneous catalyses. The catalysts are made from cheap and earth abundant cobalt metal ion. In addition, the selected porphyrin derivatives are stable, step-economy, and ease of synthetic workup. The scale-up version of heterogeneous catalysis and homogenous photocatalytic H_2 evolution prototypes from neutral water by using **3** is currently under pursuing in our group.

Acknowledgments

We thank the Ministry of Science and Technology of Taiwan and Academia Sinica for financial support.

ORCID

Chen-Hsiung Hung https://orcid.org/0000-0002-8060-348X

References

1. H. I. Karunadasa, C. J. Chang, and J. R. Long, *Nature*, **464**, 1329 (2010).
2. V. S. Thoi, Y. Sun, J. R. Long, and C. J. Chang, *Chem. Soc.Rev.*, **42**, 2388 (2013).
3. R. M. Bullock, A. M. Appel, and M. L. Helm, *Chemical Communications*, **50**, 3125 (2014).
4. C. C. L. McCrory, C. Uyeda, and J. C. Peters, *Journal of the American Chemical Society*, **134**, 3164 (2012).
5. X. Hu, B. S. Brunschwig, and J. C. Peters, *Journal of the American Chemical Society*, **129**, 8988 (2007).
6. M. M. Roubelakis, D. K. Bediako, D. K. Dogutan, and D. G. Nocera, *Energy & Environmental Science*, **5**, 7737 (2012).
7. A. E. King, Y. Surendranath, N. A. Piro, J. P. Bigi, J. R. Long, and C. J. Chang, *Chemical Science*, **4**, 1578 (2013).
8. R. S. Khnayzer, V. S. Thoi, M. Nippe, A. E. King, J. W. Jurss, K. A. El Roz, J. R. Long, C. J. Chang, and F. N. Castellano, *Energy & Environmental Science*, **7**, 1477 (2014).
9. J. G. Kleingardner, B. Kandemir, and K. L. Bren, *Journal of the American Chemical Society*, **136**, 4 (2014).
10. Y. Sun, J. P. Bigi, N. A. Piro, M. L. Tang, J. R. Long, and C. J. Chang, *Journal of the American Chemical Society*, **133**, 9212 (2011).
11. C. H. Lee, D. K. Dogutan, and D. G. Nocera, *Journal of the American Chemical Society*, **133**, 8775 (2011).
12. R. M. Kellett and T. G. Spiro, *Inorganic Chemistry*, **24**, 2373 (1985).
13. R. M. Kellett and T. G. Spiro, *Inorganic Chemistry*, **24**, 2378 (1985).
14. T. Abe, F. Taguchi, H. Imaya, F. Zhao, J. Zhang, and M. Kaneko, *Polymers for Advanced Technologies*, **9**, 559 (1998).
15. B. H. Solis, A. G. Maher, T. Honda, D. C. Powers, D. G. Nocera, and S. Hammes-Schiffer, *ACS Catalysis*, **4**, 4516 (2014).
16. D. J. Graham and D. G. Nocera, *Organometallics*, **33**, 4994 (2014).
17. M. Natali, A. Luisa, E. Iengo, and F. Scandola, *Chemical Communications*, **50**, 1842 (2014).
18. M. Natali, M. Orlandi, C. Chiorboli, E. Iengo, V. Bertolasi, and F. Scandola, *Photochemical & Photobiological Sciences*, **12**, 1749 (2013).
19. D. Huang, J. Lu, S. Li, Y. Luo, C. Zhao, B. Hu, M. Wang, and Y. Shen, *Langmuir*, **30**, 6990 (2014).
20. B. B. Beyene, S. B. Mane, and C.-H. Hung, *Chemical Communications*, **51**, 15067 (2015).
21. M. Wang, L. Chen, and L. Sun, *Energy & Environmental Science*, **5**, 6763 (2012).
22. B. H. Solis, Y. Yu, and S. Hammes-Schiffer, *Inorganic Chemistry*, **52**, 6994 (2013).
23. S. C. Marinescu, J. R. Winkler, and H. B. Gray, *Proceedings of the National Academy of Sciences of the United States of America*, **109**, 15127 (2012).
24. G. R. Geier III and J. S. Lindsey, *J. Org. Chem.*, **64**, 1596 (1999).
25. G. R. Geier III, D. M. Haynes, and J. S. Lindsey, *Org. Lett.*, **1**, 1455 (1999).
26. E. C. A. Ojadi, H. Linschitz, M. Gouterman, R. I. Walter, J. S. Lindsey, R. W. Wagner, P. R. Droupadi, and W. Wang, *The Journal of Physical Chemistry*, **97**, 13192 (1993).
27. A. D. Adler, F. R. Longo, J. D. Finarelli, J. Goldmacher, J. Assour, and L. Korsakoff, *The Journal of Organic Chemistry*, **32**, 476 (1967).
28. B. Zimmer, V. Bulach, C. Drexler, S. Erhardt, M. W. Hosseini, and A. De Cian, *New Journal of Chemistry*, **26**, 43 (2002).
29. G. A. N. Felton, R. S. Glass, D. L. Lichtenberger, and D. H. Evans, *Inorganic Chemistry*, **45**, 9181 (2006).
30. A. Wolberg and J. Manassen, *Journal of the American Chemical Society*, **92**, 2982 (1970).
31. M. Norberto, M. S. Luigi, R. Andrea, and Francesco Mallamace, *Physical Review*, **57**, 5766 (1998).
32. N. G. Connelly and W. E. Geiger, *Chemical Reviews*, **96**, 877 (1996).
33. J. P. Bigi, T. E. Hanna, W. H. Harman, A. Chang, and C. J. Chang, *Chemical Communications*, **46**, 958 (2010).

34. G. M. Jacobsen, J. Y. Yang, B. Twamley, A. D. Wilson, R. M. Bullock, M. Rakowski DuBois, and D. L. DuBois, *Energy & Environmental Science*, **1**, 167 (2008).
35. X. Hu, B. M. Cossairt, B. S. Brunschwig, N. S. Lewis, and J. C. Peters, *Chemical Communications*, 4723 (2005).
36. C. Baffert, V. Artero, and M. Fontecave, *Inorganic Chemistry*, **46**, 1817 (2007).
37. M. Razavet, V. Artero, and M. Fontecave, *Inorganic Chemistry*, **44**, 4786 (2005).
38. P.-A. Jacques, V. Artero, J. Pécaut, and M. Fontecave, *Proceedings of the National Academy of Sciences*, **106**, 20627 (2009).
39. W. R. McNamara, Z. Han, P. J. Alperin, W. W. Brennessel, P. L. Holland, and R. Eisenberg, *Journal of the American Chemical Society*, **133**, 15368 (2011).
40. J. L. Dempsey, J. R. Winkler, and H. B. Gray, *Journal of the American Chemical Society*, **132**, 16774 (2010).